Wear 303 (2013) 146–153

Contents lists available at SciVerse ScienceDirect

Wear

journal homepage: www.elsevier.com/locate/wear

# The effect of lubrication film thickness on thermoelastic instability under fluid lubricating condition

Jiaxin Zhao [a], Biao Ma [a], Heyan Li [a,*], Yunbo Yi [b]

[a] School of Mechanical Engineering, Beijing Institute of Technology, 5 South Zhongguancun Street, Haidian District, Beijing 100081, PR China
[b] Department of Mechanical and Materials Engineering, University of Denver, 2390 S. York St. Denver, CO 80208, USA

ARTICLE INFO

*Article history:*
Received 28 September 2012
Accepted 5 March 2013
Available online 14 March 2013

*Keywords:*
Thermoelastic instability
Wet clutches
Fluid lubrication
Critical speed

ABSTRACT

An idealized model consisting of a thermal conductor and a thermal insulator separated by a thin layer of lubricating fluid is developed to investigate thermoelastic instability with fluid lubrication. The governing equations are solved for the critical speed. A new dimensionless parameter $H_0$ is defined to predict the critical speed. Furthermore, the effects of various materials and the wavelength of perturbations on thermoelastic instability are discussed. It has been found that the migration speed of hot spots is nonzero, but typically very slow compared with the sliding speed and the relation between the critical speed and the fluid film thickness is non-linear. In addition, a material with low elastic modulus, low thermal expansion coefficient and high thermal conductivity will experience a high critical speed.



## 1. Introduction

Various kinds of mechanical frictional components with lubrication, such as sealing parts, bearings and clutches, are impressionable to one type of the local high temperature on the surface named hot spots which may cause a surface damage. Hot spots are caused by a type of instability during the slipping and friction process when the sliding speed is in excess of a threshold value that relies on the wavelength of the perturbation in the system. This instability, which is caused by frictional heat, elastic deformation and cooling effect, is named thermoelastic instability or TEI. This phenomenon was first introduced by Barber [1]. A theoretical model composed of two solid surfaces sliding with each other was developed to investigate TEI in frictional systems. A perturbation of the nominally uniform contact pressure on the interface of the rubbing pair will lead to a nonuniform distribution of frictional heat and a nonuniform temperature field. The subsequent thermal expansion will transform the distribution of the contact pressure in turn. This process that moves in a loop causes hot spots in some cases. A multitude of researches have been done for TEI in dry frictional systems [2–5].

For frictional parts with lubrication, the heat generation that has a significant influence on TEI makes a conspicuous difference from the non-lubricated friction. During the working process, the heat in wet frictional parts is produced totally or partly by film shearing. Though TEI may be alleviated because of not only the less quantity of heat compared with dry fiction but also the cooling effect of fluid, hot spots can still appear on friction surfaces under certain conditions. Evidence of hot spots from an experiment for wet multi-disk clutches is shown in Fig. 1, where the dark areas represent the regions that have experienced high local temperature, i.e., hot spots.

TEI in frictional systems with lubrication was first examined by Banerjee and Burton [6] who developed a theoretical model composed of a thermal conductor and an insulator sliding along the interface in the presence of a liquid lubricating film. An equation for calculating the critical speed of lubricative face type seals was proposed by Banerjee as $V_c = h_0\lambda\sqrt{K/\mu\alpha}$, where $V_c$, $h_0$, $\mu$, $\lambda$, $K$, and $\alpha$ represent the critical speed, nominal fluid film thickness, fluid viscosity, wavenumber of the perturbation, thermal conductivity and thermal expansion coefficient of metal, respectively. Then Jang and Khonsari [7–9] extend Banerjee's work by considering surface roughness.

According to their work, we may make a prediction of the critical speed for wet frictional mechanical components during fluid lubrication period. However their estimation still shows several deficiencies, e.g., their results are mainly based upon stationary wave solutions, i.e., the perturbation is presumed to be non-moving relative to the conductor. In reality, the perturbation moves at a relatively low speed with respect to the good thermal conductor, but not zero. Under an assumption of stationary perturbation, the fluid pressure and convection effects become small, therefore this assumption, non-moving perturbation, may lead to neglecting some significant impact factors on TEI and the

* Corresponding author. Tel./fax: +86 1068918085.
*E-mail address:* lovheyan@gmail.com (H. Li).

0043-1648/$ - see front matter © 2013 Elsevier B.V. All rights reserved.
http://dx.doi.org/10.1016/j.wear.2013.03.012

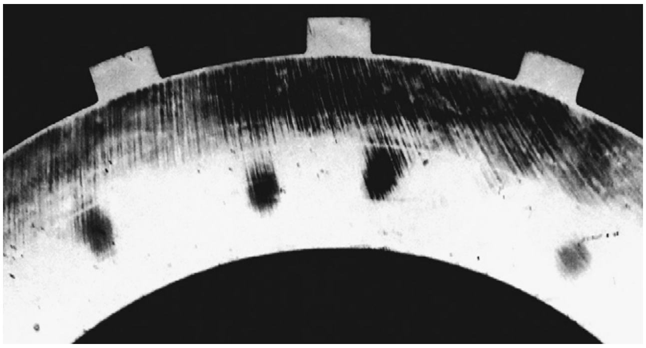

Fig. 1. Evidence of hot spots in a wet multi-disk clutch.

solution can be viewed as an approximate prediction for the critical speed.

In the current paper, we will examine the influence of lubricant film thickness on the critical speed of TEI on the basis of the moving solutions and predict a reasonable critical speed. For the purpose of evaluating the effect of finite disk thickness on TEI in the dry fiction system, Lee and Barber [3] introduced a model consisting of two semi-infinite planes and a layer with a finite thickness. Their results, which have been confirmed by Yi et al. [10], indicate that with the layer geometry there is a preferred wavelength of TEI. In an attempt to examine the effect of lubricating fluid film thickness on TEI, we introduce a fluid with finite thickness between the friction surfaces. In Lee's work, there is a minimum critical speed when $\lambda a=0.2$, where $a$ represents the half layer thickness. In this paper, we will demonstrate there is also a minimum point, which is being driven by the film thickness, on the critical speed curve.

## 2. Model

Taking the automotive wet clutch as our research object, the friction disk is often composed of a type of paper based material while the mating disk is made of steel. Since the thermal conductivity of the paper based material is about 10 times smaller than that of steel, we can make a hypothesis that the wet clutch system can be simplified as a thermal conductor–insulator system. This assumption has been adopted by Banerjee [6] and Jang [8] to examine the critical speed of the facing type seal.

A simplified schematic model is shown in Fig. 2. Following Lee's work [3], we introduce a spatially sinusoidal perturbation, moving at a speed $c$ to the positive $x$-direction, in a fluid pressure, which grows exponentially with time. More general patterns of perturbations can be obtained by means of superposition, which is equivalent to the Fourier transform. The pressure perturbation will lead to other perturbations in the system, e.g., stresses, temperature fields, fluid thickness, therefore all perturbations will have a similar expression. If we introduce a coordinate system $(x,y)$ moving with the perturbation field, the total fluid pressure can be represented as

$$p_0+\Re\{p_1\exp(bt+\imath\lambda x)\} \tag{1}$$

where $p_0$, $p_1$, $b$, and $t$ represent the unperturbed pressure, perturbed pressure, growth rate of the perturbation and time respectively, $\imath=\sqrt{-1}$.

We assume that the sinusoidal surface (conductor) moves at a speed $V$ to the positive $x$-direction while the plane surface (insulator) is stationary, as shown in Fig. 2. With respect to the two disks, the relative velocities of the perturbation are, separately, $c_1=c$ and $c_2=c-V$ to the positive $x$-direction. In order to simplify the expression of perturbations, we introduce two local

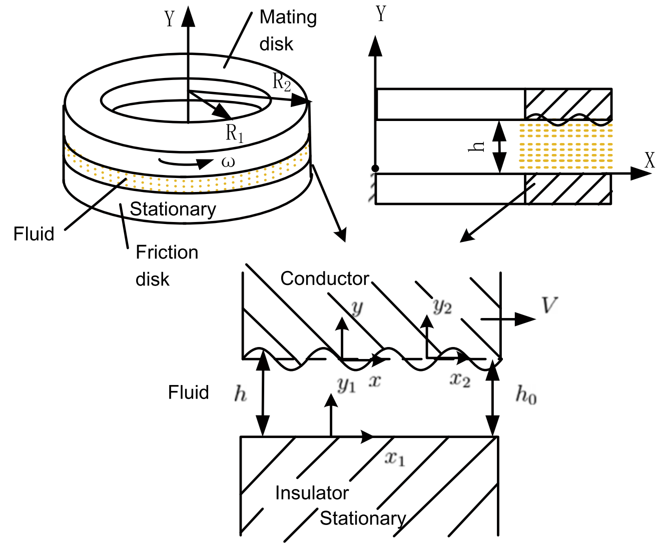


Fig. 2. Schematic diagram.

coordinate systems: $(x_1,y_1)$ and $(x_2,y_2)$ that are standing with disk 1 and disk 2 separately, as shown in Fig. 2. The relations of different coordinate systems are

$$x_1=x+c_1t, \quad x_2=x+c_2t \tag{2}$$

$$y_1=y+h_0, \quad y_2=y \tag{3}$$

$$h=h_0+\Re\{h_1\exp(bt+\imath\lambda x)\} \tag{4}$$

where $h$, $h_0$, and $h_1$ represent, respectively, the entire fluid film thickness, the nominal fluid film thickness and the perturbation of fluid film thickness.

The gap between these two surfaces is full of lubricating fluid with constant viscosity. Our research is based on the fluid lubrication condition and the influence of surface roughness is neglected. To satisfy the assumption, the fluid thickness needs to be at least three times greater than the surface roughness, i.e., $h_0 \geq 3Ra$ [8], where $Ra$ represents the surface roughness.

Some assumptions for fluid have been made: 1, the flow is laminar; 2, the gravity and inertia forces can be ignored; 3, the compressibility of fluid is negligible; 4, the fluid is Newtonian; 5, the fluid pressure is constant across the film thickness; and 6, there is no slip between the fluid and the surfaces of disks.

### 2.1. Fluid pressure and stress

In the research on fluid, we will use the local coordinate system $(x_1,y_1)$ during calculation.

#### 2.1.1. Equilibrium

On the basis of previous assumptions, the Navier–Stokes equation can be simplified to a two-dimensional equation, as

$$\frac{\partial^2 v_x}{\partial y_1^2}=\frac{1}{\mu}\frac{\partial p}{\partial x_1}, \tag{5}$$

where $v_x$, $\mu$, and $p$ are, respectively, the fluid velocity in the $x$-direction, the viscosity, and the pressure of fluid. According to Eq. (1), the pressure perturbation can be expressed as $\Re\{p_1\exp(bt+\imath\lambda(x_1-c_1t))\}$. Hence the simplified Navier–Stokes equation (5) can be rewritten as

$$\frac{\partial^2 v_x}{\partial y_1^2}=\Re\left\{\frac{\imath\lambda p_1}{\mu}\exp(bt+\imath\lambda(x_1-c_1t))\right\}. \tag{6}$$

For the purpose of facilitating the derivation process, we define a new dimensionless variable $\eta$

$$\eta=\frac{y_1}{h},\quad y_1=h\eta. \tag{7}$$

Solving Eq. (6), we can obtain

$$v_x(x_1,\eta)=\Re\left\{C\eta+D+\left(\frac{\imath h^2\lambda p_1\eta^2}{2\mu}+A\eta+B\right)\exp(bt+\imath\lambda(x_1-c_1t))\right\} \tag{8}$$

Since $p_1$ is already a first order perturbation term, we can replace $h$ by a zero order term $h_0$.

As the insulator is stationary and the conductor is moving at a speed $V$ to the positive $x$-direction, the boundary conditions of fluid flow are $v_x(x_1,0)=0$, $v_x(x_1,1)=V$, which imply

$$D+\Re\{B\exp(bt+\imath\lambda(x_1-c_1t))\}=0 \tag{9}$$

$$C+\Re\left\{\left(\frac{\imath h_0^2\lambda p_1}{2\mu}+A\right)\exp(bt+\imath\lambda(x_1-c_1t))\right\}=V \tag{10}$$

giving

$$A=-\frac{\imath h_0^2\lambda p_1}{2\mu},\quad B=0,\quad C=V,\quad D=0. \tag{11}$$

Hence, the solution of the fluid velocity is

$$v_x(x_1,\eta)=\Re\left\{V\eta-\left(\frac{\imath h_0^2\lambda p_1\eta(1-\eta)}{2\mu}\right)\exp(bt+\imath\lambda(x_1-c_1t))\right\}. \tag{12}$$

### 2.1.2. Continuity

The total fluid flow passing a given control volume is

$$q(x_1)=\int_0^h v_x(x_1,y_1)\,dy_1=h\int_0^1 v_x(x_1,\eta)\,d\eta \tag{13}$$

where $q$ represents the volume rate of flow in unit time. Neglecting the second order of the perturbation and substituting Eq. (12) into Eq. (13), the fluid flow can be written as

$$q(x_1)=\Re\left\{\frac{V}{2}\left[h_0+h_1\exp(bt+\imath\lambda(x_1-c_1t))\right]-\left(\frac{\imath h_0^3\lambda p_1}{12\mu}\right)\exp(bt+\imath\lambda(x_1-c_1t))\right\} \tag{14}$$

We consider a small control volume shown in Fig. 3, the volume of which is $h\Delta$. Since the sinusoidal surface is moving at a speed $V$ to the positive $x$-direction, the control volume is decreasing at a rate

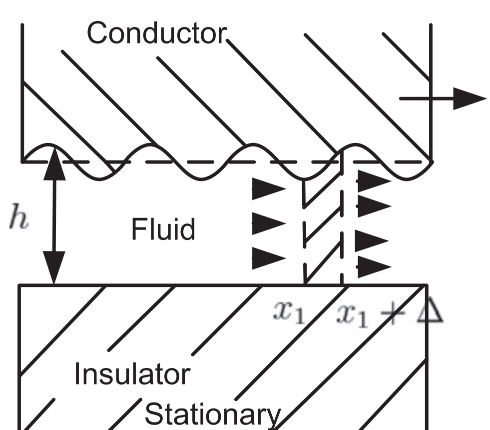


**Fig. 3.** Fluid flow and continuity.

$$V\Delta\frac{\partial h}{\partial x_1}. \tag{15}$$

Since the fluid is incompressible, the flow rate out of this volume must exceed that into it, implying

$$q(x_1+\Delta)-q(x_1)=V\Delta\frac{\partial h}{\partial x_1} \tag{16}$$

and hence

$$\frac{\partial q}{\partial x_1}=V\frac{\partial h}{\partial x_1}. \tag{17}$$

Substituting $q$ from Eq. (14), then we have the pressure perturbation as

$$p_1=\frac{6\imath\mu Vh_1}{\lambda h_0^3} \tag{18}$$

Hence, the perturbation of normal stress on the boundary between the conductor and the fluid is

$$\sigma_1(y=0)=-\Re\{p_1\exp(bt+\imath\lambda x)\}=-\Re\left\{\frac{6\imath\mu Vh_1}{\lambda h_0^3}\exp(bt+\imath\lambda x)\right\}. \tag{19}$$

Substituting the pressure perturbation (18) into Eq. (12), the velocity of fluid can be written as

$$v_x(x_1,\eta)=\Re\left\{V\eta+\left(\frac{3h_1V\eta(1-\eta)}{h_0}\right)\exp(bt+\imath\lambda(x_1-c_1t))\right\}. \tag{20}$$

### 2.1.3. Shear traction

On the basis of Newton's Law of Viscosity, the relation between the shear traction and the fluid velocity can be expressed as (neglecting second and higher order terms)

$$\tau_1=\mu\frac{\partial v_x}{\partial y_1}=\mu\frac{\partial v_x}{\partial\eta}\frac{\partial\eta}{\partial y_1}=\mu\Re\left\{\frac{V}{h_0}+\frac{2h_1V(1-3\eta)\exp(bt+\imath\lambda(x_1-c_1t))}{h_0^2}\right\}. \tag{21}$$

In particular, at the interface where $\eta=1$, the shear stress is

$$\tau_1(y=0)=-\Re\left\{\frac{4\mu Vh_1\exp(bt+\imath\lambda x)}{h_0^2}\right\}. \tag{22}$$

## 2.2. Fluid heat flow

The perturbation of viscous heat dissipated in the fluid can be expressed as [8]

$$Q_1=\mu\int_0^h\left(\left(\frac{\partial v_x}{\partial y_1}\right)^2-\left(\frac{dv_0}{dy_1}\right)^2\right)dy_1=-\Re\left\{\frac{2\mu V^2h_1}{h_0^2}\exp(bt+\imath\lambda(x_1-c_1t))\right\} \tag{23}$$

where $v_0$ denotes the unperturbed velocity term, $v_0=(Vy_1)/h_0$. During the calculation, we neglect the second and higher order of the perturbation.

Owing to the assumption that the friction disk is an insulator, all heat fluxes would flow into the mating disk. Hence the heat flux on the interface is

$$Q_1(y=0)=-\Re\left\{\frac{2\mu V^2h_1}{h_0^2}\exp(bt+\imath\lambda x)\right\} \tag{24}$$

### 2.3. Temperature field and heat flux in fluid

A suitable form for temperature perturbation in the fluid can be written as [6]

$$T_1(x_1,y_1)=\Re\{(T_A+T_By_1+T_Cy_1^2)\exp(bt+\imath\lambda(x_1-c_1t))\} \tag{25}$$

Hence the perturbation of heat flux in the fluid can be expressed as

$$Q_1=-K_f\frac{\partial T_1}{\partial y_1}=-\Re\{K_f(T_B+2T_Cy_1)\exp(bt+\imath\lambda(x_1-c_1t))\} \tag{26}$$

where $K_f$ is the thermal conductivity of fluid. At the boundary between the conductor and the fluid, neglecting second and higher order terms, the perturbations of temperature field and heat flux can be expressed as, respectively,

$$T_1(y=0)=\Re\{(T_A+T_Bh_0+T_Ch_0^2)\exp(bt+\imath\lambda(x_1-c_1t))\} \tag{27}$$

$$Q_1(y=0)=-\Re\{K_f(T_B+2T_Ch_0)\exp(bt+\imath\lambda(x_1-c_1t))\} \tag{28}$$

Meanwhile, since all dissipated heat flow into the conductor, the value of heat flux perturbation at the interface between the insulator and fluid must be zero, implying

$$Q_1(y=-h)=-\Re\{K_fT_B\exp(bt+\imath\lambda(x_1-c_1t))\}=0 \tag{29}$$

### 2.4. Temperature field and heat flux in the conductor

In the research on the conductor, we will use the local coordinate system $(x_2,y_2)$ during calculation. The temperature field in the conductor must satisfy the heat conduction equation

$$\frac{\partial^2T}{\partial x_2^2}+\frac{\partial^2T}{\partial y_2^2}=\frac{1}{k}\frac{\partial T}{\partial t} \tag{30}$$

where $k$ represents the thermal diffusivity of the conductor

$$k=\frac{K}{\rho c_p} \tag{31}$$

$K$, $\rho$, and $c_p$ are the thermal conductivity, the density, and the specific heat of the conductor, respectively. We can assume that the temperature perturbation can be expressed as

$$T_2(y_2)=\Re\{F(y_2)\exp(bt+\imath\lambda(x_2-c_2t))\} \tag{32}$$

Substituting this equation into Eq. (30) and solving it, with the boundary condition $y_2\to\infty$, $T_2\to 0$, we can obtain a suitable form of the temperature field perturbation [3]

$$T_2(y_2)=\Re\{T_0\exp(-my_2)\exp(bt+\imath\lambda x)\} \tag{33}$$

where

$$m=\sqrt{\lambda^2+\frac{\gamma}{k}},\quad \gamma=b-\imath\lambda c_2 \tag{34}$$

$T_0$ is an unknown constant.

Accordingly, the heat flux perturbation at the interface between the lubricating fluid and the conductor is

$$Q_2(y=0)=-K\frac{\partial T_2}{\partial y_2}(y_2=0)=\Re\{KT_0m\exp(bt+\imath\lambda x)\} \tag{35}$$

### 2.5. Perturbation of film thickness

Then we consider the temperature and heat flux boundary conditions at the interface, which can be written as

$$y=0:\quad T_1=T_2,\quad Q_1=Q_2;\quad y=-h:\quad Q_1=0 \tag{36}$$

Combined with Eqs. (24) and (27)–(29), the perturbation of the fluid film thickness can be solved as

$$h_1=\frac{h_0^2KmT_0}{2\mu V^2} \tag{37}$$

Consequently, the perturbation of the fluid pressure can be rewritten as

$$\Re\left\{\frac{3\imath KmT_0}{\lambda h_0V}\exp(bt+\imath\lambda(x_1-c_1t))\right\}. \tag{38}$$

Those equations imply that when the nominal fluid film thickness $h_0$ increases, the perturbation of the film thickness $h_1$ increases accordingly. Meanwhile, the perturbation of the fluid pressure decreases with increasing $h_0$. These two opposite effects on the perturbations may lead to a phenomenon that when the nominal film thickness equals a particular value, the friction system will be most sensitive to TEI, i.e., the critical speed will become minimal. This prediction will be testified in Section 3.

Furthermore, the energy balance equation on the interface can be written as

$$-\Re\left\{\frac{2\mu V^2h_1}{h_0^2}\exp(bt+\imath\lambda x)\right\}=\Re\{KT_0m\exp(bt+\imath\lambda x)\} \tag{39}$$

### 2.6. Thermoelastic stresses and displacements

For a thermoelastic problem, the normal displacements and stresses can be obtained by superposing a particular solution corresponding to a strain function $\psi$ [11, Chapter 22] to the isothermal solutions A and D of Green and Zerna [12], as

$$u_y=\frac{1}{2G}\frac{\partial\psi}{\partial y}+\frac{1}{2G}\frac{\partial\phi}{\partial y}+\frac{1}{2G}\left(y\frac{\partial\omega}{\partial y}-(3-4\nu)\omega\right) \tag{40}$$

$$\sigma_y=-\frac{\partial^2\psi}{\partial x^2}-\frac{\partial^2\phi}{\partial x^2}+y\frac{\partial^2\omega}{\partial y^2}-2(1-\nu)\frac{\partial\omega}{\partial y} \tag{41}$$

$$\tau_{xy}=\frac{\partial^2\psi}{\partial x\partial y}+\frac{\partial^2\phi}{\partial x\partial y}+y\frac{\partial^2\omega}{\partial x\partial y}-(1-2\nu)\frac{\partial\omega}{\partial x} \tag{42}$$

where $u_y$, $\sigma_y$, and $\tau_{xy}$ represent, respectively, the displacement in the $y$-direction, the normal stress in the $y$-direction and the shear stress. The parameter $\phi$, $\omega$ and strain function $\psi$ can be expressed as [3]

$$\phi=\Re\{M\exp(\imath\lambda x-\lambda y)\} \tag{43}$$

$$\omega=\Re\{N\exp(\imath\lambda x-\lambda y)\} \tag{44}$$

$$\psi=\Re\left\{\frac{\beta T_0}{m^2-\lambda^2}\exp(bt+\imath\lambda x-my)\right\} \tag{45}$$

where $M$ and $N$ are the arbitrary complex constants and $\beta$ can be written as

$$\beta=\frac{2G\alpha(1+\nu)}{1-\nu} \tag{46}$$

where $\alpha$, $G$, and $\nu$ represent, respectively, the thermal expansion coefficient, the shear modulus, and Poisson's ratio of the conductor.

Substituting Eqs. (43)–(45) into (40)–(42), we can obtain the thermal normal displacements and stress at the interface as

$$u_y(0)=\Re\left\{\frac{m\beta T_0}{2G(\lambda^2-m^2)}\exp(bt+\imath\lambda x)-\left(\frac{M\lambda}{2G}+\frac{(3-4\nu)N}{2G}\right)\exp(\imath\lambda x)\right\} \tag{47}$$

$$\sigma_y(0)=\Re\left\{-\frac{\lambda^2\beta T_0}{\lambda^2-m^2}\exp(bt+\imath\lambda x)+\left(M\lambda^2+2(1-\nu)N\lambda\right)\exp(\imath\lambda x)\right\} \tag{48}$$

$$\tau_{xy}(0)=\Re\left\{\frac{i\lambda m\beta T_0}{\lambda^2-m^2}\exp(bt+\imath\lambda x)-(\imath M\lambda^2+\imath(1-2\,\nu)N\lambda)\exp(\imath\lambda x)\right\} \tag{49}$$

With regard to a TEI problem, all the perturbations in the system have the same growth rate $b$, e.g. perturbations can be expressed as $\Re\{f(y)\exp(bt+\imath\lambda x)\}$. When the relative velocity of the rubbing pair is less than the critical speed, the exponential growth rate $b<0$ and all the perturbations will die out with time. In contrast, the system will become unstable ($b>0$) on condition that the relative velocity exceeds the critical speed. Thus we can calculate the speed threshold when the exponential growth rate $b=0$. At the interface, the perturbations in the displacement, the fluid film thickness, the normal stress, and the shear stress, must equal each other, thus the mechanical boundary conditions are

$$u_y(0)=h_1,\quad \sigma_y(0)=\sigma(y=0),\quad \tau_{xy}(0)=\tau(y=0)$$

With Eqs. (19), (22) and (47)–(49) plus the heat transfer boundary condition equation (39), we can construct the homogeneous equations as

$$\mathbf{SU}=0$$

where

$$\mathbf{S}=\begin{bmatrix} -1 & \frac{-\lambda}{2G} & -\frac{3-4\nu}{2G} & \frac{m\beta}{2G(\lambda^2-m^2)} \\ \frac{6\mu V}{\lambda h_0^3} & \lambda^2 & 2(1-\nu)\lambda & -\frac{\beta\lambda^2}{\lambda^2-m^2} \\ \frac{4\mu V}{h_0^2} & -\imath\lambda^2 & -\imath(1-2\nu)\lambda & \frac{\imath\beta\lambda m}{\lambda^2-m^2} \\ -\frac{2\mu V^2}{h_0^2} & 0 & 0 & -mK \end{bmatrix}$$

$$\mathbf{U}=(h_1\ \ M\ \ N\ \ T_0)'$$

In the next step, we transform the calculation to an eigenvalue problem by presenting a necessary condition of the linear equations existing a non-zero solution that the determinant of the coefficient matrix must equal zero, i.e., $\det(\mathbf{S})=0$. Hence we can obtain a complex equation as

$$\imath\lambda^3 mKh_0^3G+(2(m(2\nu-1)K+\imath\beta(-1+\nu)V)V\mu+\imath m^2KGh_0^2)h_0\lambda^2 +4mK\mu((\nu-\tfrac{1}{2})h_0m-\tfrac{3}{2}\ \nu+\tfrac{3}{2})V\lambda-6\mu Vm^2K(-1+\nu)=0 \tag{50}$$

Then we define the following dimensionless parameters in efforts to rewrite Eq. (50) in a dimensionless form

$$m^*=\frac{m}{\lambda},\quad V^*=\frac{V}{k\lambda} \tag{51}$$

$$c_2^*=\frac{c_2}{k\lambda},\quad \beta^*=\frac{k\beta}{K} \tag{52}$$

$$H=h_0\lambda,\quad H_0=\frac{h_0^2\lambda\sqrt{G}}{\sqrt{\mu k}} \tag{53}$$

The dimensionless determinant can be expressed as

$$\imath m^*HH_0^2+2H(m^*V^*(2\nu-1)H^2+\imath H^2V^{*2}\beta^*(\nu-1)+\tfrac{1}{2}\imath H_0^2m^{*2}) +2V^*m^*H(Hm^*(2\nu-1)-3(\nu-1))-6HV^*m^{*2}(\nu-1)=0 \tag{54}$$

When the growth rate $b=0$, we assume the dimensionless parameter $m^*$ as

$$m^*=\sqrt{1-\imath c_2^*}=\xi+\imath\zeta \tag{55}$$

We may notice that the sign of $c_2^*$ stands for the direction of the migration speed, so changing it has no effect on the absolute value of our results. Hence we make an assumption that the dimensionless migration speed $c_2^*<0$. Under this situation, $\xi$ and $\zeta$ can be expressed as

$$\xi=\sqrt{\tfrac{1}{2}(1+\sqrt{1+(c_2^*)^2})} \tag{56}$$

$$\zeta=\sqrt{\tfrac{1}{2}(-1+\sqrt{1+(c_2^*)^2})} \tag{57}$$

Then we can separate the real and imaginary parts of Eq. (54), both of which must equal zero. Hence we can obtain two real numbers as

$$2V^*H[(H(2\nu-1)-3(\nu-1))(\xi+\xi^2-\zeta^2)]-H_0^2\zeta(1+2\xi)=0 \tag{58}$$

$$2V^*H[HV^*\beta^*(\nu-1)+\zeta(1+2\xi)(H(2\nu-1)-3(\nu-1))] +H_0^2(\xi+\xi^2-\zeta^2)=0 \tag{59}$$

For given values of all the system parameters, the nominal film thickness $h_0$ and the wavenumber of the perturbation $\lambda$, the dimensionless critical speed $V^*$ and the dimensionless migration speed $c_2^*$ can be solved by those two equations.

## 3. Results

Steel is almost always used for the mating disks in wet plate clutches, the values of the material parameters for a widely used steel are shown in Table 1. Furthermore, we select a typical lubricating fluid, the viscosity of which is 0.0968 Pa s.

In order to satisfy our fluid lubrication assumptions, the nominal fluid film thickness $h_0 \geq 3Ra$. An experiment has been designed for the purpose of obtaining the surface roughness of a wet clutch during different using stages. The experimental data are shown in Table 2. On the basis of Table 2, the nominal film thickness $h_0 \geq 15$ μm. Hence, we assign three different values for the fluid film thickness, which are $h_0=20$ μm, 30 μm, 40 μm, and solve Eqs. (58) and (59) to obtain the dimensionless critical speed $V^*$ and the dimensionless migration speed $c_2^*$. The results are shown in Figs. 4 and 5, respectively.

According to Fig. 4, two significant conclusions can be deduced. Primarily, the critical speed is within the range of the working speed of wet clutches. If we assume the film thickness $h_0=40$ μm and the wavenumber $\lambda=40(1/\text{m})$, the critical speed would be 6.7 m/s, which equals 640 RPM on condition that the mean radius of the disk is 0.1 m. That critical speed is within the limits of the working speed of most wet clutches, so the clutch can experience TEI during the working process and hot spots will appear if the process is long enough. This conclusion accords with our

**Table 1**
Material properties of the conductor.

| Material | $E$ (N/m$^2\times10^{11}$) | $\nu$ | $\alpha$ (°C$^{-1}\times10^{-5}$) | $K$ (W/m °C) | $k$ (m$^2$/s $\times10^{-5}$) |
|---|---|---|---|---|---|
| Steel | 1.6 | 0.29 | 1.27 | 45.9 | 1.208 |
| Cast iron | 1.25 | 0.25 | 1.2 | 54 | 1.298 |

**Table 2**
Surface roughness of the mating disk.

| Engagement times | 0 | 100 | 500 | 800 | 1000 | 1500 |
|---|---|---|---|---|---|---|
| Roughness (μm) | 4.0632 | 3.1687 | 2.5168 | 2.5918 | 2.4911 | 2.2543 |

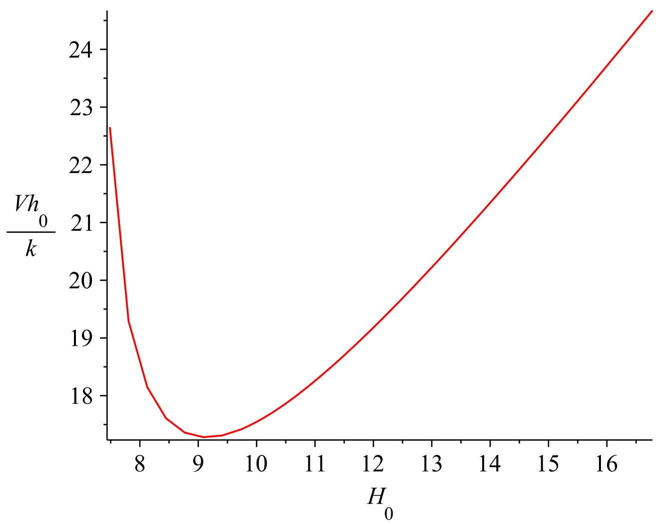


**Fig. 4.** The relation between the dimensionless critical speed and $H_0$.

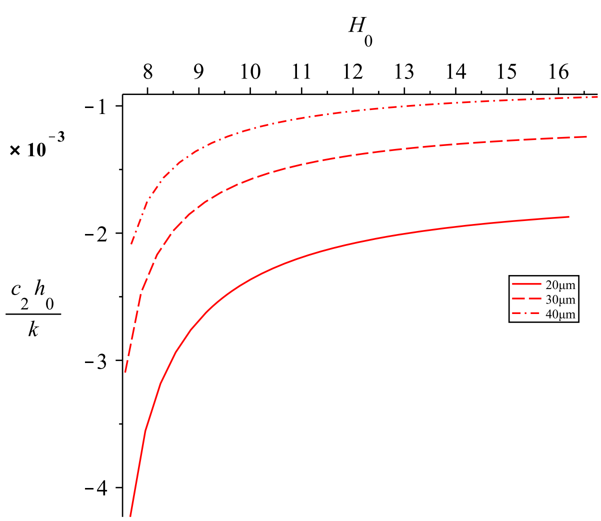


**Fig. 5.** The relation between the dimensionless migration speed and $H_0$.

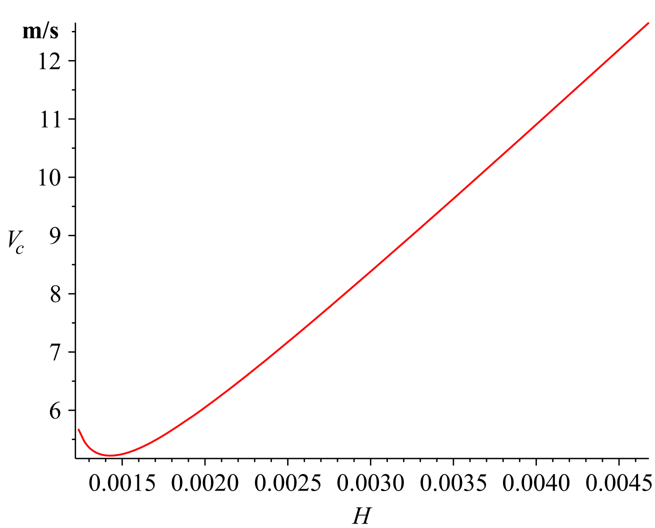


**Fig. 6.** The dimensional critical speed.

experimental result that hot spots would occur in time of regular operations.

Secondly, for a given value of the fluid film thickness, it is conspicuously that the critical speed changes with the wavenumber (or the wavelength) of the perturbation. Additionally, there is a minimum point for the curve when the wavelength equals a preferred value. In other words, when the dimensionless parameter $H_0$ equals a preferred value, i.e., $h_0^2\lambda$ equals a particular value, the minimum critical speed will occur. This curve implies that the system will become unstable under a perturbation with a particular wavelength on condition that the film thickness is fixed.

On the basis of Fig. 4, the minimum dimensionless critical speed occurs at about $H_0{=}9.2$ on the curve. Consequently, we can predict that the fluid film thickness has a similar effect on TEI as the disk thickness, which is a significant factor for TEI testified by Lee and Barber [3].

Fig. 5 shows that the migration speed is indeed very small compared with the critical speed, but not zero. It demonstrates that the stationary solution, which is based on the assumption that the migration speed is zero, is not accurate for TEI with fluid lubrication. Furthermore, it is obvious that the migration speed decreases with the enhancement of $H_0$, which means the stationary solution would be more reasonable when $H_0$ is large.

In contrast, we compare our result with Barnejee's [6] critical speed equation $V_c = h_0\lambda\sqrt{K/\mu\alpha}$. In his equation, the critical speed is a linear function of the dimensionless parameter $H = h_0\lambda$. A relationship between $H$ and the critical speed $V_c$ is shown in Fig. 6, which implies that $V_c$ would become a linear function when $H$ is sufficiently large. Hence, Figs. 5 and 6 can explain the reason why our moving wave solution would become a linear function as Banerjee and Burton's stationary wave solution [6] on condition that $H_0$ is large enough.

### 3.1. The effect of wavelength

According to Fig. 4, the critical speed is a function of $H_0$. For a given lubricating fluid thickness $h_0$, the dimensionless parameter $H_0$ is proportional to the wavenumber $\lambda$, or inversely proportional to the wavelength $l$, as

$$H_0 = \frac{h_0^2\lambda\sqrt{G}}{\sqrt{\mu k}} = \frac{2\pi}{l}\frac{h_0^2\sqrt{G}}{\sqrt{\mu k}} \tag{60}$$

Hence

$$l = \frac{2\pi}{H_0}\frac{h_0^2\sqrt{G}}{\sqrt{\mu k}} \tag{61}$$

where $l$ represents both the wavelength and the spacing between hot spots on the mating disk in the unstable state.

Fig. 4 shows that the critical speed has a minimum value when $H_0 \approx 9.2$, demonstrating that the first thermoelastic instability is caused by a perturbation that has a wavelength as $l \approx 1.57 \times 10^8 h_0^2$ according to Eq. (61).

In our theoretical model, we construct an assumption that the size in the $x$-direction is infinite, which means that the circumference of the mating disk must be long enough, i.e., that must be longer than the wavelength of the perturbation. This restriction can be expressed as

$$\frac{2\pi}{l_M}\frac{h_0^2\sqrt{G}}{\sqrt{\mu k}} < H_0 \tag{62}$$

where $l_M$ represents the circumference of the mating disk.

### 3.2. The effect of the fluid film thickness

During the actual working process of wet plate clutches, the fluid film thickness is ever changing that has influence on the critical speed. Therefore we will examine another important factor, the film thickness. To find out the relationship between the film thickness and the critical speed, we substitute some given values of wavenumber $\lambda = 40{,}50{,}60(1/\mathrm{m})$ into Eqs. (58) and (59). Then choosing steel shown in Table 1 as the material of the conductor and fluid viscosity as $\mu = 0.0968$ Pa s, we can obtain the critical speed shown in Fig. 7. That figure illustrates that the system preferred wavelength under which the critical speed is minimal is determined by a given value of film thickness. In addition, the system preferred number of hot spots is changing in time of the working process since the film thickness varies.

From those curves in Fig. 7, we can conclude that the minimum point of the dimensionless critical speed $V/k\lambda$ varies with the wavelength or the wavenumber of the perturbation. Moreover, as shown in Fig. 4, when the dimensionless parameter $H_0$ equals some preferred values, the minimum critical speed will occur. Hence, we can predict the critical speed depending on $H_0$.

### 3.3. The effect of the material parameters

For different materials, such as steel and cast iron, the elastic modulus, thermal conductivity and thermal expansion coefficient may vary. In order to select an optimal material for the clutch system, engineers must consider comprehensively of size, performance, service life and stability in the design phase. Since thermoelastic instability is a significant contributor to impact on wet clutches, we will examine the effect of different materials on TEI. In contrast, we select the cast iron as an alternative material for the conductor, and values of its parameters are shown in Table 1. The fluid viscosity is maintained as 0.0968 Pa s. Then we define $h_0 = 40\ \mu$m and make an comparison between different materials of the mating disk, i.e. steel and cast iron, as shown in Fig. 8.

It is obvious that the critical speed of cast iron is higher than that of steel, which implies cast iron is a better material to avoid TEI for wet clutches. Then we will examine the effect of material properties on the critical speed to find out the reason why cast iron is better.

*Elastic modulus*. A low elastic modulus can help alleviate the non-uniformity of the contact pressure distribution, hence decreases the tendency of TEI. This conclusion has been confirmed by both Anderson [13] with the experimental method and Zagrodzki [14] with the analytical study.

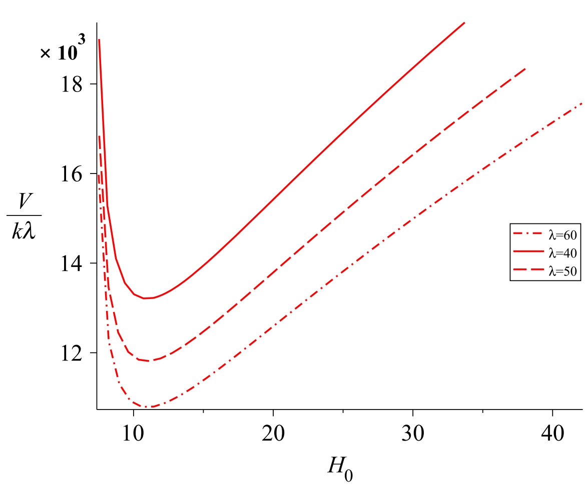


**Fig. 7.** The effect of the fluid film thickness on the critical speed.

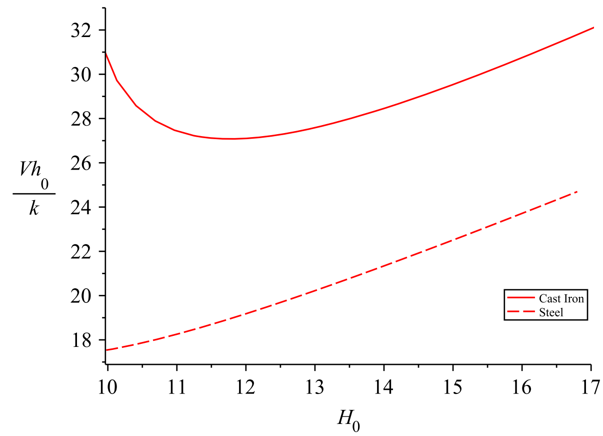


**Fig. 8.** The critical speed for steel and cast iron.

*Thermal expansion coefficient*. A small thermal expansion coefficient has a similar effect as the elastic modulus to help alleviate the non-uniformity of the contact pressure distribution. The reason is that with the same temperature rise, materials with lower thermal expansion coefficient will experience smaller expansion that keeps contact pressure more uniform.

*Thermal conductivity*. The thermal conductivity has an opposite effect on the critical speed as the elastic modulus, which means that a large thermal conductivity will lead to an increase of the critical speed. Consequently, increasing the thermal conductivity helps reduce the non-uniformity of the contact pressure distribution. This prediction has been confirmed by Anderson's experimental work [13].

### 3.4. Finite thickness problem

Those predictions made in the previous sections were based on a semi-infinite plane model while real clutch disks have a finite thickness. This approximation will fail if the actual thickness of the disk is small compared with the spatial decay rate of temperature, namely, when the real part of $ma$ is far less than 1 ($\Re(ma) \ll 1$). We assume $\lambda = 40(1/\mathrm{m})$, $h_0 = 40\ \mu$m, and $a = 1$ mm, and choose other parameters shown in Table 1, then substitute those values into Eqs. (58) and (59), obtaining $c_2^* = -0.6$. Consequently, the migration speed $c_2 = c_2^* k\lambda = -2.9 \times 10^{-4}$ m/s. With Eq. (34), when the growth rate $b = 0$, we can obtain

$$ma = a\sqrt{\lambda^2 + \frac{-\imath\lambda c_2}{k}} = 0.042 + 0.012\imath \qquad (63)$$

Since $\Re(ma) = 0.042 \ll 1$, we can conclude our semi-infinite plane model is acceptable and our predictions are reasonable.

## 4. Conclusions

A theoretical model is developed to investigate thermoelastic instability in a frictional system with fluid lubrication that is simplified as a thermal conductor–insulator frictional system. A semi-infinite plane model has been testified to be reasonable for investigating TEI in wet clutches.

Governing equations are established and solved for the threshold of the velocity named the critical speed beyond which TEI occurs. We can conclude that TEI occurs in wet clutches during the working process. In addition, the migration speed of hot spots is typically very slow compared with the sliding speed, but not zero.

The relation between the critical speed and the fluid film thickness is non-linear.

A new dimensionless parameter $H_0$ is introduced to help us predict the critical speed. For a thermal conductor–insulator system with fluid lubrication, the dimensionless critical speed $Vh_0/k$ is determined by $H_0$, and has a minimum value when $H_0$ equals a preferred value.

The effects of different materials of the conductor (mating disk) on TEI are also discussed. We can conclude that a material with low elastic modulus, low thermal expansion coefficient and high thermal conductivity will experience a high critical speed.

## Acknowledgements

Authors would like to appreciate for the helpful support given by Prof. J.R. Barber at the University of Michigan. Authors would also acknowledge the financial support by National Natural Science Foundation of China (No. 51175042).

## References

[1] J.R. Barber, The influence of thermal expansion on the friction and wear process, Wear 10 (1967) 155–159.
[2] T.A. Dow, R.A. Burton, Thermoelastic instability of sliding contract in the absence of wear, Wear 19 (1972) 315–328.
[3] K.J. Lee, J.R. Barber, Frictionally excited thermoelastic instability in automotive disk brakes, ASME Journal of Tribology 115 (1993) 607–614.
[4] P. Decuzzi, M. Ciavarella, G. Monno, Frictionally excited thermoelastic instability in multi-disk clutches and brakes, ASME Journal of Tribology 123 (2001) 865–871.
[5] S.W. Lee, Y.H. Jang, Effect of functionally graded material on frictionally excited thermoelastic instability, Wear 267 (2009) 1715–1722.
[6] B.N. Banerjee, R.A. Burton, An instability for parallel sliding of solid surfaces separated by a viscous liquid film, ASME Journal of Lubrication Technology (1976) 157–166.
[7] J.Y. Jang, M.M. Khonsari, Thermoelastic instability including surface roughness effects, ASME Journal of Tribology 121 (1999) 648–654.
[8] J.Y. Jang, M.M. Khonsari, Thermoelastic instability with consideration of surface roughness and hydrodynamic lubrication, ASME Journal of Tribology 122 (2000) 725–732.
[9] J.Y. Jang, M.M. Khonsari, A generalized thermoelastic instability analysis, Proceedings of the Royal Society of London 459 (2003) 309–329.
[10] Y.B. Yi, J.R. Barber, P. Zagrodzki, Eigenvalue solution of thermoelastic instability problems using fourier reduction, Proceedings of the Royal Society Series A 456 (2000) 2799–2821.
[11] J.R. Barber, Elasticity, 3rd ed., Springer, 2010.
[12] A.E. Green, W. Zerna, Theoretical Elasticity, Clarendon Press, 1954.
[13] A.E. Anderson, R.A. Knapp, Hot spotting in automotive friction systems, in: International Conference on Wear of Materials, vol. 2, 1989, pp. 673–680.
[14] P. Zagrodzki, Analysis of thermomechanical phenomena in multidisc clutches and brakes, Wear 140 (1990) 291–308.